

Ferro uidity in a two-component dipolar Bose-Einstein Condensate

Hiroki Saito¹, Yuki Kawaguchi², and Masahito Ueda^{2,3}

¹Department of Applied Physics and Chemistry, University of Electro-Communications, Tokyo 182-8585, Japan

²Department of Physics, University of Tokyo, Tokyo 113-0033, Japan

³ERATO Macroscopic Quantum Project, JST, Tokyo 113-8656, Japan

(Dated: February 21, 2024)

It is shown that the interface in a two-component Bose-Einstein condensate (BEC) in which one component exhibits a dipole-dipole interaction spontaneously forms patterns similar to those formed in a magnetic liquid subject to a magnetic field. A hexagonal pattern, hysteretic behavior, and soliton-like structure are numerically demonstrated. A phenomenon similar to the labyrinthine instability is also found. These phenomena may be realized using a ^{52}Cr BEC. The periodic density modulation in the superfluid ground state offers evidence of supersolidity.

PACS numbers: 03.75.Mn, 03.75.Hh, 47.65.Cb

When a magnetic liquid (a colloidal suspension of magnetic nanoparticles) is subjected to a magnetic field perpendicular to the surface, the liquid is magnetized and the surface undergoes spontaneous deformation into characteristic patterns shaped like 'horns' growing from the liquid. This surface instability is known as the normal-field or Rosensweig instability [1] and is the subject of active research [2, 3, 4, 5, 6, 7, 8]. The system also exhibits a variety of phenomena, such as hysteretic behaviors [4], transition between hexagonal and square patterns [5], and stabilization of a soliton-like structure [8]. Because of the visual appeal of the pattern formation, the dynamics of the magnetic-liquid surfaces are introduced even in art [9].

In the present Letter, we show that a Bose-Einstein condensate (BEC) of an atomic gas with a strong dipole-dipole interaction [10] exhibits instabilities and pattern formations similar to those in magnetic liquids. The system considered here is schematically illustrated in Fig. 1. A two-component BEC is used, in which the atoms in component 1 have a magnetic dipole moment and the atoms in component 2 are nonmagnetic. A magnetic field is applied to x the direction of the fully polarized magnetic dipole (say, in the z direction). A magnetic-field gradient in the z direction pulls the atoms in component 1 in the z direction, and then the two components are phase-separated for a strong field gradient. The surface deformation in a magnetic liquid by the Rosensweig instability occurs when it lowers the sum of gravitational, surface, and magnetic energies [3]. In analogy with a magnetic-liquid system, the field gradient plays the role of gravity, and the quantum pressure and contact interaction create an interface energy, corresponding to the surface tension of a magnetic liquid.

A two-component BEC is used because in order for the density pattern to be formed in a single-component BEC, the dipole-dipole interaction must overcome the contact interaction, which leads to dipolar collapse [11]. In fact, the parameter region in which a biconcave density pattern is formed is in the immediate vicinity of the

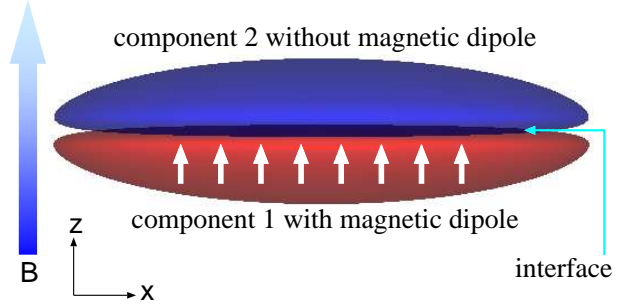


FIG. 1: (Color) Schematic illustration of the system. A two-component BEC is confined in a trapping potential, in which component 1 has a magnetic dipole moment and component 2 does not. The magnetic dipole is polarized in the z direction by the magnetic field. The two components are phase-separated due to the field gradient $dB/dz < 0$.

region of the collapse instability [12, 13]. In Refs. [14, 15], quasi-two-dimensional (2D) systems are considered in order to avoid the collapse, and 2D solitons are shown to be stabilized by the dipolar interaction. Using a multi-component BEC is another possible way of realizing pattern formation without suffering a dipolar collapse, since texture formation is much easier than density-pattern formation. For example, spin domains can be formed by a small spin-dependent interaction [16].

In this Letter we show that a hexagonal pattern of density peaks emerges on the interface between nonmagnetic and fully polarized ^{52}Cr BECs [10]. We find that the number of peaks can be controlled by the strength of the field gradient. Hysteresis also occurs between flat and single-spike interfaces, which resembles soliton-like structures in magnetic liquids [8]. We show that various patterns are formed, including a labyrinthine pattern [17].

We consider a two-component BEC described by the macroscopic wave functions ψ_1 and ψ_2 in the zero-temperature mean-field approximation. The wave functions obey the nonlocal Gross-Pitaevskii (GP) equations

given by

$$i\hbar \frac{\partial \psi_1}{\partial t} = \frac{\hbar^2 \nabla^2}{2M_1} \psi_1 + V_1 \psi_1 + \frac{dB}{dz} z \psi_1 + g_{11} |\psi_1|^2 + g_{12} \psi_1 \psi_2^* + U(r) \psi_1 + \int_{-\infty}^{\infty} U(r-r') |\psi_1(r')|^2 dr' \psi_1; \quad (1a)$$

$$i\hbar \frac{\partial \psi_2}{\partial t} = \frac{\hbar^2 \nabla^2}{2M_2} \psi_2 + V_2 \psi_2 + g_{22} |\psi_2|^2 + g_{12} \psi_1 \psi_2^* + U(r) \psi_2 + \int_{-\infty}^{\infty} U(r-r') |\psi_2(r')|^2 dr' \psi_2; \quad (1b)$$

where M_n and V_n are atomic mass and trap potential for component $n = 1$ or 2 . The interaction coefficients are given by $g_{nn^0} = 2\hbar^2 a_{nn^0}/M_{nn^0}$ with a_{nn^0} and M_{nn^0} being the s -wave scattering length and the reduced mass between components n and n^0 . The dipole-dipole interaction has the form $U(r) = \mu_0^2 (1 - 3z^2/r^2)/(4\pi r^3)$, where μ_0 is the permeability of vacuum and μ is the magnetic dipole moment of the atoms in component 1. For simplicity, we assume that the two components have the same mass M and the same number of atoms $N=2$ and that they experience the same axisymmetric harmonic potential given by $V_n = M\omega^2[(\frac{1}{2}(x^2 + y^2) + \frac{1}{2}z^2)]$, where ω_x and ω_z are radial and axial trap frequencies. Gravity only shifts the origin and can be neglected. The magnetic field depends only on z , and dB/dz is uniform. We employ the $m_J = -3$ magnetic sublevel of a ^{52}Cr atom for component 1, for which $\mu = 6\mu_B$ with μ_B being the Bohr magneton and $a_{11} = 100a_B$ [18] with a_B being the Bohr radius. We assume $a_{11} = a_{22} = a_{12}$.

We first study stable states of the system, obtained by replacing i with 1 on the left-hand sides of Eq. (1). The numerical propagation is performed using the Crank-Nicolson scheme and the dipolar part is calculated using a fast Fourier transform. The initial state of the imaginary-time propagation is a flat-interface state $\psi_n = \psi_n + r_n$, where r_n represents a small complex number randomly chosen on each mesh. The small noise is added to break the axisymmetry of the system.

Figure 2 (a) shows an isodensity surface of component 1 for $a_{11} = a_{22} = a_{12} = 100a_B$ and $dB/dz = 600 \text{ mG/cm}$. The hexagonal mountain-like pattern on the interface between the two components is similar to the Rosensweig pattern on a magnetic-liquid surface. Since the density is high and hence the dipole-dipole interaction is large at the center of the trap, the peaks around the center are higher than those on the periphery. Figure 2 (b) shows the column-density profiles integrated along the z axis. It is interesting that the left and middle panels of Fig. 2 (b) exhibit phase separation in the x - y plane, even though the scattering lengths do not satisfy the immiscible condition. This is because the density of component 1 is large at the peaks due to the dipole-dipole interaction, which repels component 2. In fact, the total density [right panel of Fig. 2 (b)] also has a hexagonal pattern.

When the field gradient becomes tight, the number and

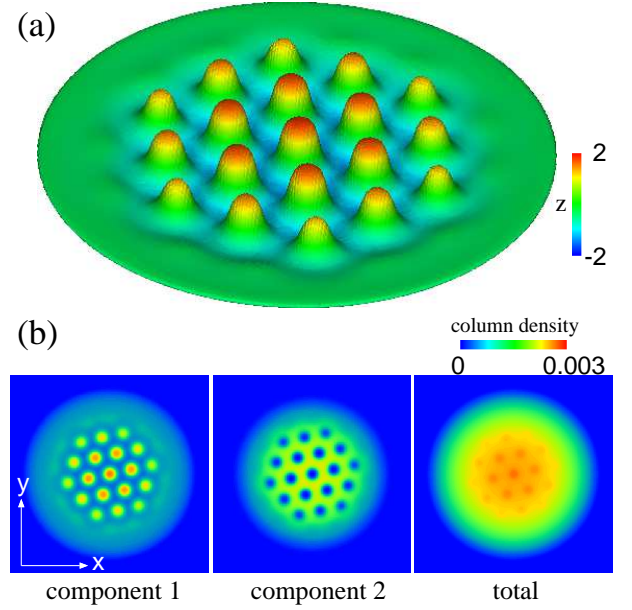


FIG. 2: (Color) Stable state of the two-component dipolar BEC for $a_{11} = a_{22} = a_{12} = 100a_B$ and $\mu = 6\mu_B$ in an axisymmetric potential with $(\omega_x; \omega_z) = (2; 100/800) \text{ Hz}$. The number of atoms is $N = 4 \times 10^6$ with an equal population in each component and the field gradient is $dB/dz = 600 \text{ mG/cm}$. (a) Isodensity surface of component 1. The color represents the z coordinate normalized by $(\hbar/M\omega_z)^{1/2}$. (b) Column densities $\int |\psi_1|^2 dz$, $\int |\psi_2|^2 dz$, and $\int (|\psi_1|^2 + |\psi_2|^2) dz$ normalized by $N M \omega_z / \hbar$. The field of view is $50 \times 50 \mu\text{m}$.

height of the peaks decrease and eventually the interface becomes flat. The appearance and disappearance of the pattern exhibits hysteresis with respect to a change in the field gradient. Figure 3 (a) depicts stable states obtained from the imaginary-time propagation of the GP equation as $\mu B/dz$ is increased or decreased. When $\mu B/dz$ is increased from a small value [red arrow in Fig. 3 (a)], the hexagonal pattern of the peaks changes into a single peak, which then disappears at $dB/dz = 1054 \text{ mG/cm}$. On the other hand, when $\mu B/dz$ is decreased from a large value [blue arrow in Fig. 3 (a)], the interface remains flat until $dB/dz = 1028 \text{ mG/cm}$. Therefore, there is a bistable region at $\mu B/dz = 1028\text{--}1054 \text{ mG/cm}$, in which the single-peak state and the flat-interface state are both stable. In the bistability region, the energies of the two states are almost degenerate. Such hysteretic behavior has been predicted [3, 7] and observed [4, 8] for magnetic liquids, in which the applied magnetic field and hence the magnetization is changed. For a wider pancake-shaped BEC, bistability between the flat-surface and hexagonal-peak states may be observed as in a magnetic liquid.

The single-peak structure in the bistable region in Fig. 3 (a) is similar to the "ferrosoliton" [8] in a magnetic liquid, which shows a stable soliton-like peak. Figure 3 (b) shows the density profile of the cross section of the single-peak state at $dB/dz = 1040 \text{ mG/cm}$. A round

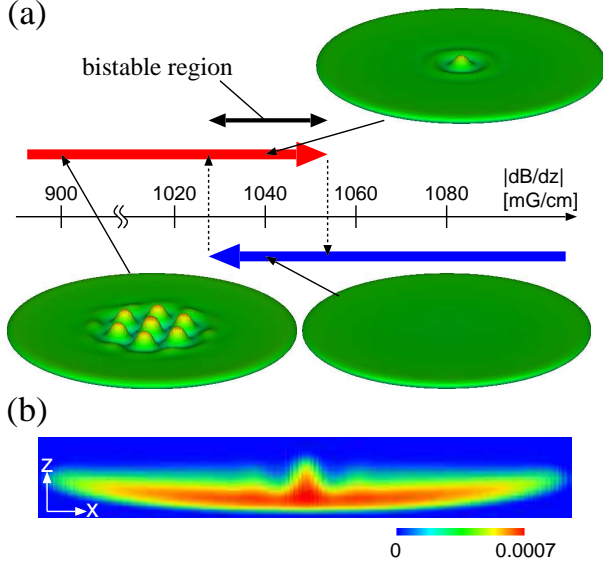


FIG. 3: (Color) (a) Hysteresis with respect to a change in the field gradient. The red and blue arrows indicate that a single-peak or flat interface is stable for $|dB/dz| < 1054$ mG/cm or $|dB/dz| > 1028$ mG/cm. Beyond these thresholds, the two stable states convert to each other (dotted arrows). The isodensity surfaces are shown for $|dB/dz| = 900$ and 1040 mG/cm. (b) Density profile of the cross section on the $y = 0$ plane for the single-peak state at $|dB/dz| = 1040$ mG/cm. The field of view is 44×6.7 μm and the density is normalized by $N(M\lambda_2/h)^{3/2}$. The parameters are the same as those in Fig. 2 except for $|dB/dz|$.

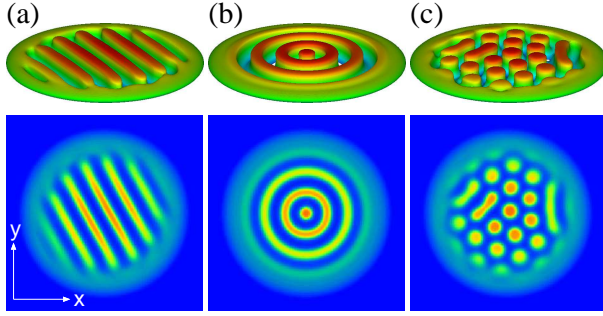


FIG. 4: (Color) Isodensity surface (upper figures) and column density (lower panels) of component 1 for various stable states. The difference in (a)–(c) is only in the initial perturbations in the imaginary-time propagation. The field gradient is $|dB/dz| = 200$ mG/cm. The other parameters and the color scales are the same as those in Fig. 2.

the peak, the interface oscillates in a concentric manner, as in the ferrosoliton in a magnetic liquid [8].

To investigate various metastable patterns, we apply initial perturbations to trigger the pattern formation. Figure 4 (a) is obtained by applying an additional magnetic field $\propto \sin(k_x x + k_y y)$ for $t < 1$ μs in the imaginary-time propagation, where $k_x a_2 = \pi/3$ and $k_y a_2 = 1$ with $a_2 = (h/M\lambda_2)^{1/2}$. We find that the imaginary-time

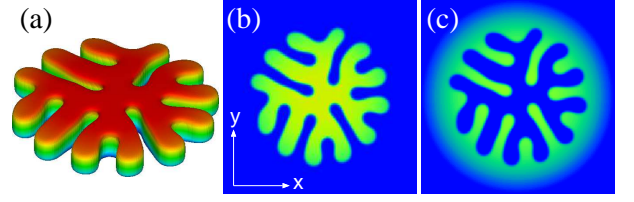


FIG. 5: (Color) (a) Isodensity surface of component 1 and column density of (b) component 1 and (c) component 2 for $a_{11} = 100a_B$, $a_{12} = a_{22} = 120a_B$, $|dB/dz| = 0$, and $N = 8 \times 10^6$. The other conditions and the color scales are the same as those in Fig. 2.

propagation relaxes the system to the stripe pattern as shown in Fig. 4 (a). This pattern is robust against small additional noise. The initial temporary magnetic field for Fig. 4 (b) is $\propto \cos(\sqrt{x^2 + y^2}/a_2)$. The concentric pattern in Fig. 4 (b) is stable against axisymmetry-breaking noise. Figure 4 (c) is obtained without an additional magnetic field, with only a small noise added to the initial state. These results imply that there are many metastable states with various patterns. In Fig. 4 (c), the peaks partly merge into each other. The merging of the peaks tends to occur for a large dipole interaction and small field gradient. For $|dB/dz| = 600$ mG/cm, the stripe and concentric patterns in Figs. 4 (a) and 4 (b) are unstable against forming peaks. Although the square lattice of the peaks is found to be unstable for the parameters in Figs. 2 and 4, a hexagonal-square-lattice transition may occur for other parameters, as in magnetic liquids [3, 5].

Figure 5 shows a stable state for $|dB/dz| = 0$ which has an intricate pattern similar to the labyrinthine pattern in a thin layer of magnetic liquid confined with an immiscible nonmagnetic liquid [17]. The relation between the labyrinthine instability in a magnetic liquid [2] and that in the present system remains to be clarified.

Next we study the dynamics of the pattern formation in a nondissipative system by solving the real-time propagation of Eq. (1). Figure 6 shows the time evolution of the system, where the initial state is a flat-interface state for $|dB/dz| = 1200$ mG/cm, as shown in Fig. 6 (a). In order to break the axisymmetry, a small initial noise is added to the initial state. We let the system evolve in time with $|dB/dz| = 600$ mG/cm, for which the stable state has hexagonal peaks, as shown in Fig. 2 (a). The density fluctuations grow into many peaks, as in Figs. 2 (b) and 2 (c), due to the Rosensweig instability. We note that the characteristic wavelength in the pattern at the early stage [Fig. 2 (b)] is smaller than that in the later pattern [Fig. 2 (c)]. This difference indicates that the most unstable wavelength in the linear regime does not correspond to the final stable pattern determined by the nonlinear interaction. A similar situation also occurs in magnetic liquids [6]. If the phenomenological dissipation

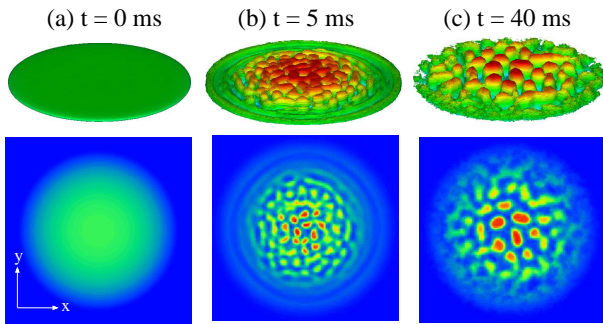


FIG. 6: (Color) Time evolution of the isodensity surface (upper figures) and column density (lower panels) of component 1. The initial state is the at-interface state for $\delta B = \delta z = 1200 \text{ mG/cm}$ and the field gradient changes to $\delta B = \delta z = 600 \text{ mG/cm}$ at $t = 0$. The field of view is $50 \times 50 \text{ m}$. The parameters and color scales are the same as those in Fig. 2.

is taken into account by replacing i with $i - 0.03$ [19] in Eq. (1), the hexagonal pattern is formed at 50 ms .

A candidate for component 2 is the $^7\text{S}_3$ $m_J = 0$ state of a ^{52}Cr atom. Though the $m_J = \pm 3$ states are unstable against dipolar collisions, the lifetime is long enough (ns) [10] to observe the pattern-formation dynamics. The spin exchange dynamics, such as $m_J = 0 + 0 \rightarrow \pm 3 + \pm 3$, can be suppressed using, e.g., the microwave-induced quadratic Zeeman effect [21]. The scattering lengths measured in Ref. [18] give $a_{22} \approx 60.7a_B + a_0 = 7$ and $a_{12} \approx 67.8a_B$, with a_0 being the scattering length for the colliding channel with total spin 0, which is unknown. The scattering length a_{11} can be controlled using the magnetic Feshbach resonance [20]. The inhomogeneity of the magnetic field $1 \text{ G/cm} = 10 \text{ m}$ is much smaller than the resonance width 1.7 G [18]. We can therefore obtain $a_{11} \approx a_{22} \approx a_{12} \approx 60a_B$ by changing a_{11} , if $\hbar\omega_0$ is not very large. We have confirmed that the Rosensweig pattern emerges for these scattering lengths. Another possibility for component 2 is an alkali atom, for which, however, a_{12} has not been measured yet. The pattern formation for various scattering lengths merits further study.

An important difference between the present system and magnetic liquids is that the present system is a superfluid, while a conventional magnetic liquid is a normal fluid. In the Rosensweig pattern, the total density shows a periodic modulation (i.e., diagonal order), while the present system by construction possesses an off-diagonal order, presenting strong evidence of supersolidity. Another difference is that the present system is fully polarized irrespective of the strength of the magnetic field, while the magnetic liquid is paramagnetic. The difference between a compressible gas and an incompressible liquid is also important. It is remarkable that both systems exhibit similar phenomena despite these differences.

In conclusion, we have studied pattern formation on

the interface in a two-component BEC, in which one component exhibits a dipole-dipole interaction. We found a rich variety of interfacial patterns, including Rosensweig hexagonal peaks and a labyrinthine pattern. We also observed hysteretic behavior and the ferrosoliton, as in magnetic liquids. We expect that the two-component system proposed here will provide a new insight into surface and interface physics with long-range interactions.

This work was supported by MEXT Japan (KAKENHI No. 17071005 and No. 20540388, and the Global COE Program "the Physical Sciences Frontier") and by the Matsuo Foundation.

-
- [1] M. D. Cowley and R. E. Rosensweig, *J. Fluid Mech.* **30**, 671 (1967).
 - [2] R. E. Rosensweig, *Ferrohydrodynamics* (Cambridge Univ. Press, Cambridge, 1985) and references therein.
 - [3] A. Gailitis, *J. Fluid Mech.* **82**, 401 (1977).
 - [4] J.-C. Bacri and D. Salin, *J. Phys. Lett.* **45**, 559 (1984).
 - [5] D. Allais and J.-E. Wesfreid, *Bull. Soc. Fr. Phys. Suppl.* **57**, 20 (1985).
 - [6] A. Lange, B. Reimann, and R. Richter, *Phys. Rev. E* **61**, 5528 (2000).
 - [7] R. Friedrichs and A. Engel, *Phys. Rev. E* **64**, 021406 (2001).
 - [8] R. Richter and I. V. Barashenkov, *Phys. Rev. Lett.* **94**, 184503 (2005).
 - [9] S. Kodama and M. Takeno, *SIGGRAPH 2001, Electronic Art and Animation Catalog*, pp. 138.
 - [10] A. Griesmaier, J. Werner, S. Hensler, J. Stuhler, and T. Pfau, *Phys. Rev. Lett.* **94**, 160401 (2005).
 - [11] T. Lahaye, J. Metz, B. Frohlich, T. Koch, M. Meister, A. Griesmaier, T. Pfau, H. Saito, Y. Kawaguchi, and M. Ueda, *Phys. Rev. Lett.* **101**, 080401 (2008).
 - [12] K. Goral, K. Rzaewski, and T. Pfau, *Phys. Rev. A* **61**, 051601(R) (2000).
 - [13] R. M. Wilson, S. Ronen, J. L. Bohn, and H. Pu, *Phys. Rev. Lett.* **100**, 245302 (2008).
 - [14] P. Pedri and L. Santos, *Phys. Rev. Lett.* **95**, 200404 (2005).
 - [15] I. Tikhonov, B. A. Malomed, and A. Vardi, *Phys. Rev. Lett.* **100**, 090406 (2008).
 - [16] J. Stenger, S. Inouye, D. M. Stamper-Kurn, H.-J. Miesner, A. P. Chikkatur, and W. Ketterle, *Nature (London)* **396**, 345 (1998).
 - [17] L. T. Romankiw, M. M. G. Slusarczyk, and D. A. Thompson, *IEEE Trans. Mag.* **11**, 25 (1975).
 - [18] J. Werner, A. Griesmaier, S. Hensler, J. Stuhler, T. Pfau, A. Simon, and E. Tiesinga, *Phys. Rev. Lett.* **94**, 183201 (2005).
 - [19] M. Tsubota, K. Kasamatsu, and M. Ueda, *Phys. Rev. A* **65**, 023603 (2002).
 - [20] T. Lahaye, T. Koch, B. Frohlich, M. Fattori, J. Metz, A. Griesmaier, S. Giovanazzi, and T. Pfau, *Nature (London)* **448**, 672 (2007).
 - [21] S. R. Leslie, J. Guzman, M. Vengalattore, J. D. Sau, M. L. Cohen, and D. M. Stamper-Kurn, *arXiv:0806.1553*.